MINISTRY OF EDUCATION AND SCIENTIFIC RESEARCH
National University of Science and Technology POLITEHNICA Bucharest
Faculty of Industrial Engineering and Robotics

Alexandru VASILE

DOCTORAL THESIS

-SUMMARY-

Configuration of metamaterial cores used for sandwich structural components

Scientific coordinator,

Professor **Dan Mihai CONSTANTINESCU**

- 2025 -

THE COMMITTEE FOR THE DOCTORAL THESIS

President		National University of Science and Technology POLITEHNICA Bucharest
Scientific coordinator	Professor Dan Mihai CONSTANTINESCU	
Referent	Professor Mircea Cristian DUDESCU	Technical University of Cluj-Napoca
Referent	Professor Amado George ȘTEFAN	Military Technical Academy „Ferdinand I”
Referent	Professor Gheorghe Gabriel JIGA	National University of Science and Technology POLITEHNICA Bucharest

CONTENTS

INTRODUCTION 2
CHAPTER 1 - ANALYSIS OF MECHANICAL METAMATERIALS TYPES......................6
CHAPTER 2 DEFINITION OF THE GEOMETRIC MODEL OF SANDWICH STRUCTURES WITH MECHANICAL METAMATERIALS CORES 8
CHAPTER 3 COMPRESSIVE TESTING OF THE PROPOSED METAMATERIAL SAMPLES 13
CHAPTER 4 NUMERICAL SIMULATION OF COMPRESSION TESTS 17
CHAPTER 5 LOW SPEED IMPACT TESTING...21
CHAPTER 6 FINAL CONCLUSIONS 25
6.1 General conclusions 25
6.2 Personal contributions...27
6.3 Future research...28
BIBLIOGRAPHY 30

INTRODUCTION

Motivation for choosing the research topic

The development of sandwich structures has its origins in the 20th century aerospace and naval engineering, where lightweight yet high-strength materials were needed to ensure structural efficiency. Traditional sandwich configurations, consisting of two rigid faces and a lightweight inner layer, initially used honeycomb or foam cores to improve flexural stiffness and energy absorption. With advances in materials science, additive manufacturing (AM), and computational design (CAD), mechanical metamaterial cores have become an attractive alternative, offering superior performance through customized topology and programmable behaviour. The research community's interest in this topic has grown in the 21st century due to the potential of metamaterials to achieve unprecedented mechanical behaviours, such as negative Poisson's ratios, high impact energy dissipation and absorption, and tuneable anisotropy. As a result, the convergence of modelling and fabrication of very small complex topologies and the possibility of their experimental and numerical validation has propelled the exploration of these novel innovative artificial architectures, making them a prominent area of interdisciplinary research.

Current challenges include optimizing and minimizing defects during the fabrication of such structures, improving mechanical robustness under complex loading conditions, and increasing the ability to parameterize and scale such geometries. In addition, understanding the long-term durability and deformation mechanisms of sandwich configurations with novel topologies remains a critical area of research. Also, advanced modelling and simulation methods are needed to effectively predict the mechanical behaviour of metamaterials, with a view to structural optimization from the design phase. The motivation behind the choice of the thesis research topic arose from the need to address these challenges through interdisciplinary research and exploration of the multifunctionality of metamaterial-based sandwich structures, such as vibration damping and energy absorption, in order to increase the interest in their wide-scale adoption in engineering.

Relevance and importance of the doctoral research

Whether incorporated into sandwich components or not, metamaterials constitute a current research direction in the field of unconventional structural elements, being artificial materials designed to exhibit unusual properties or behaviours. Although the notion is mature enough to expect intense research in the mechanical field, it has only experienced significant interest in recent decades, with the advances in imaging technologies and the development of additive manufacturing capabilities. These tools have transformed the means available to researchers in various fields, providing more efficient control over the manufacturing scale and allowing the exploitation of new geometric configurations and material design. At the same time, the idea of modifying the micro-geometry of a structure in order to obtain a macroscopic behaviour adapted to a specific application has been developed [1].

From metamaterial structures with constant cross-section, such as hexagonal honeycombs or chiral topology, to complex three-dimensional geometries, such as interconnected ligament cores, foams, or foldable walls, all have seen a long exposure to research and implementation in practical applications. In addition, with the progress of additive manufacturing technologies, very complex topologies can now be generated and analysed with methods involving an automated approach. More detailed classifications of the types of existing sandwich structures with metamaterial cores are presented in [2–4].

The intensive use in many critical applications, together with the existence of several components in the basic construction, has favoured the analysis of the design freedoms of such configurations. There are a multitude of types of cores and faces that can be used, and the choice of materials depends on the specific requirements of each application. The performance of the panels is influenced by factors such as the nature and physical properties of the component elements, the interaction between them, the ratios of the defining geometric features, etc. For example, honeycomb cores are often used in aerospace applications due to their high strength-to-weight ratio, while foam cores are commonly used in the construction industry due to their low cost and good insulation properties.

Systematic studies of various mechanical properties of the most common types of metamaterials, such as [5–8], can provide valuable indications on the possible applications of such topologies. The modification of the mechanical response of the structures, such as the energy absorption capacity and the overall stability of the structure, can be done by changing the dimensions and orientation of the representative volume element (RVE) or by using a gradient-based approach. Relevant articles for understanding how different modifications of the basic geometry affect the mechanical properties are [9], [10], [11], [12].

Additive manufacturing techniques, such as selective laser melting (SLM) [13,14], direct metal laser sintering (DMLS) [15,16] and stereolithography (SLA) [17,18], have already been demonstrated to be suitable for creating complex topologies from metals, polymers or ceramics. General observations on the fabrication parameters of each method are summarized in studies such as [19,20]. Ongoing research aims to refine the fabrication parameters to achieve higher resolution, reduce defects and improve mechanical properties, while investigating new materials and hybrid bonding approaches to improve the performance and scalability of metamaterial structures.

The traditional method of developing mechanical metamaterials involves a heuristic approach, in which artificial materials are developed and tested manually, to be confirmed or disproven as a viable option for certain implementation directions. Often, they are not built based on clear rules regarding the basic configuration of a sandwich structure. Thus, the lack of restrictions on the number of materials, number of faces, fabrication parameters, macro- or micro-level geometry and the way the materials are interfacing gives rise to an endless selection of combinations of existing or conceivable topologies, and associated materials or fabrication technologies.

Thus, there is a need to establish rules based on which to simplify the choice of the type of geometry used. Among these are the way in which the structure will be used, the intensity of the anticipated stresses during its lifetime and the profitability of the materials used. In addition, it is useful to establish a methodology that starts from the choice of the type of sandwich configuration and the core used and ends by obtaining the mechanical properties relevant for a given application, taking into account all aspects related to the manufacture, testing and simulation of the behaviour of the structural component.

Thus, based on the multitude of scientific papers published each year in this field and the desire to identify innovative solutions for high-performance lightweight structures, the topic of the doctoral thesis becomes relevant and can help stimulate research interest in this direction.

Purpose and objectives of the doctoral research

The main goal of the work is to develop a methodology that involves the design, fabrication and testing of new configurations of sandwich structures with cores formed by mechanical metamaterials, which can be easily integrated into physical components, whether we are talking about classic sandwich configurations that are used in predetermined areas, or whether we are talking about their incorporation into stand-alone pieces by using shell-type elements.

To achieve this goal, the doctoral thesis aims to achieve the following main objectives:

1. Studying the specialized literature in order to identify the most promising metamaterial topologies used in sandwich configurations, as well as the applicable fabrication and testing methods.
2. Configuring sandwich structures that incorporate metamaterial cores formed by new, clearly defined and easily parameterizable representative cells.
3. Fabricating the proposed configurations and investigating the quality of the obtained samples, by highlighting probable manufacturing defects and ways to avoid them.
4. Testing the specimens in uniaxial compression and identifying general deformation modes, as well as estimating the mechanical properties at other relative density values.
5. Exploring and characterizing some modifications of the designed cells, to validate the easy parameterization of the proposed topologies and studying how they influence the mechanical properties.
6. Using finite element analysis to predict the mechanical behaviour of the studied structures and making a comparison between the results obtained and experimental data.
7. Studying the response of structures to low-velocity impact loads, as well as methods for increasing energy absorption performance.

Structure of the doctoral thesis

The doctoral thesis is structured in six chapters, accompanied by bibliographical references.

Chapter 1 presents a review of the specialized literature, which provides context and highlights existing research in the field of mechanical metamaterials. The existing configurations relevant for cores and sandwich composites are detailed, observations on their applications and properties, information on the additive manufacturing techniques used, as well as destructive and non-destructive testing procedures for the designed structures.

Chapter 2 develops a set of general rules that formed the basis for the design of representative cells of new triple periodic minimum surfaces (TPMS) and stochastic metamaterials, the way in which they were defined, and a preliminary analysis of the possibilities of additive printing, constructive parameters and anisotropy. Subsequently, the material properties and the SLA manufacturing procedure adopted for the production of the specimens are detailed, as well as various control methods: analysis of dimensional deviations, surface quality and homogeneity.

The uniaxial compression testing of the 10 types of sandwich specimens printed from photopolymer resin is presented in chapter 3. The experimentally determined failure mechanism is detailed for each specimen, by comparison with the gyroid geometry, used as a reference topology. Subsequently, the repeatability of the tests is analysed and how the mass distribution in the volume of the part can influence the way in which the structures deform. In addition, a method is presented by which the mechanical properties can be estimated for multiple values of the relative density based on experimental data, how the alteration of the initially proposed uniform geometries influences the behaviour of the structures, as well as the mechanical response of the specimens to cyclic compressive stresses is developed.

In chapter 4, the numerical analysis of the compression tests is developed. The characteristics of implicit geometric modelling are presented and how the models obtained by this technique can be integrated into numerical simulations. Subsequently, four types of material models are presented, the boundary conditions, the discretization of geometries and how they influence the results obtained. Finally, the deviations between the results of the finite element analysis and the data obtained through experimental tests are detailed.

The analysis of the low-velocity impact behaviour of the proposed topologies, both simple and with bi-component silicone filling, is made in chapter 5. Also, a method is developed for filling the voids in the sample volume so as to ensure their homogeneity. Finally, the parameters evaluated following the impact tests and the results obtained following the stresses at two different impact energies, on 10 sandwich structures, are presented.

Chapter 6 contains the essential conclusions of the thesis, the contributions made, the limitations encountered and possible directions for future research.

CHAPTER 1 - ANALYSIS OF MECHANICAL METAMATERIALS TYPES

Mechanical metamaterials offer a high degree of freedom in terms of design, from the types of materials, to the geometry used, to the ways of combining the elements that compose a sandwich structure, to the way of interfacing them, to the additional filling components that can be used. This, although it seems advantageous, can induce a continuous search for perfect models that is costly in time and financial resources. It is important to narrow the search area, based on favourable observations of previous research so as to reach the most promising results as quickly as possible.

Additive manufacturing processes, although conceptually seem very accessible, are difficult to use in order to obtain parts free of defects, which present repeatability in terms of their testing. Knowing the influence of manufacturing parameters can improve the results and their consistency.

Attributing a failure mode to mechanical metamaterials is difficult, as several types of stresses are observed that lead to the destruction of the samples. In addition to the significant influences of manufacturing defects, metamaterials can have a “bending dominated” or “stretching dominated” behaviour, depending on the strongest stresses occurring in the component elements, bending moments or axial loads. In general, the bending-dominated deformation mechanism makes the structures ideal for energy absorption, while the tensile-dominated structures tend to be more rigid.

Many research works have studied the axial load, bending and impact responses of metamaterials in their raw form or of sandwich structures with two-dimensional cores, but very few have verified the behaviour of three-dimensional configurations. Examples of such topologies are shown in Fig. 1-1Fig. 1-1. Consequently, it is evident that research in the field of using three-dimensional mechanical metamaterials in the form of a core in sandwich applications is not sufficiently developed to increase the degree of confidence in this type of materials and lead to their adoption in industrial applications.

Formatted: Font: 12 pt, Not Bold

Formatted: Font: 12 pt, Not Bold, Not Italic, Check spelling and grammar

Formatted: Font: 12 pt, Not Bold

Formatted: Font: 12 pt, Not Bold, Not Italic, Check spelling and grammar

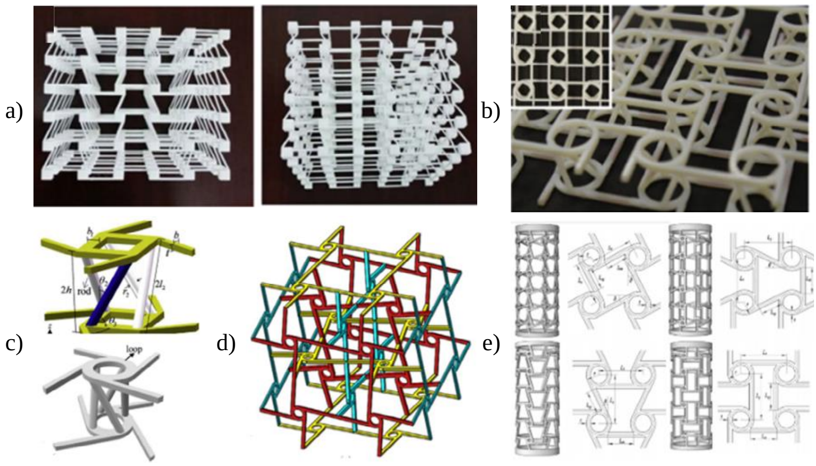

f)

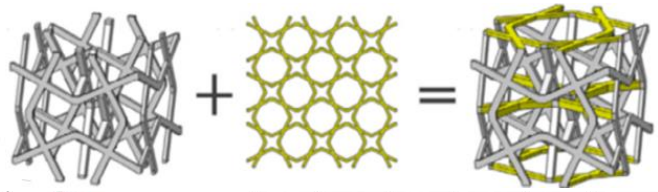

g)

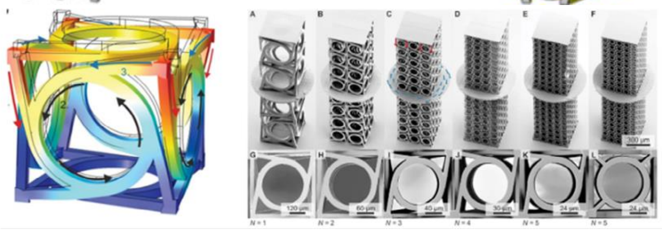

Fig. 1-1 Metamaterial topologies 3D [21], [22], [23], [24], [25]

Thus, after consulting the current state of existing metamaterial structures and performing an analysis of how they can be manufactured, I believe that a suitable direction of research is the prototyping of new three-dimensional mechanical metamaterial configurations, through manufacturing processes belonging to different categories of technologies. In addition to the aspects often encountered in the literature, an analysis of printed samples must be carried out to identify manufacturing defects that can induce errors in the interpretation of the behaviour of metamaterials. This can be done either by testing a significant number of samples to observe the repeatability of the results, or by precise three-dimensional scanning of the structures and interpreting the identified problems. It is also possible to try to achieve structures with variable relative density, with different gradients, so that the density is maximum near the high load areas and minimum in the low-load areas. Finally, after experimental testing, it is recommended to verify the results by comparison with numerical simulations, although this step can be problematic given the complex geometries and the interaction between different materials. If a computational analysis is impossible, it is advisable to identify a practical application that incorporates the proposed configurations, so as to perform efficient testing.

CHAPTER 2 DEFINITION OF THE GEOMETRIC MODEL OF SANDWICH STRUCTURES WITH MECHANICAL METAMATERIALS CORES

Following the analysis carried out in the first chapter on the types of existing metamaterials and their characteristics, in conjunction with the available manufacturing possibilities, a set of rules was defined, intended to simplify the choice of the main research direction. Based on this, eight new topologies of TPMS-type structures were defined, together with the gyroid geometry selected as a reference element, given that it has been intensively studied in the specialized literature. In addition, a stochastic geometry was also defined, intended to simulate a behaviour specific to foams. The mathematical expressions of the proposed topologies are presented in Table 2-1~~Table 2-1~~.

Table 2-1 Mathematical functions describing the topologies of the analysed samples

Sample	Function	
S1	$f(x,y,z) = cos(x)\,sin(y) + cos(y)\,sin(z) + cos(z)\,sin\,(x)$	(2-1)
S2	$\mathrm{f(x,y,z) = 2[cos(x)\,cos(y) + cos(x)\,cos(z) + cos(z)\,cos\,(y)] - [cos(2x) + cos(y) + cos\,(2z)]}$	(2-2)
S3	$f(x,y,z) = cos(x)\,cos(y) + cos(x)cos(z) + cos\,(y)cos(z) + sin(x)cos(y) + sin(x)cos(z) + sin(y)cos\,(z) + sin(y)cos(z) + sin\,(z)cos(x) + sin\,(z)cos(y)$	(2-3)
S4	$\mathrm{f(x,y,z) = cos(2x)\,cos(y)cos(z) + cos(2y)\,cos(x)\,cos(z) + cos(2z)\,cos(x)\,cos(y) + sin(x)\,cos(y) + sin(x)\,cos(z) + sin(y)\,cos(z) + sin(y)\,cos(z) + sin(z)\,cos(x) + sin(z)\,cos(y)}$	(2-4)
S5	$f(x,y,z) = sin(x)\,cos(y)\frac{z}{2} + sin(y)\,cos(z)\frac{x}{2} + sin(z)\,cos(x)\frac{y}{2}$	(2-5)
S6	$\mathrm{f(x,y,z) = 4cos(x)cos(y)cos(z) - (cos(2x)cos(2y) + cos(2y)cos(2z) + cos(2x)cos(2z))}$	(2-6)
S7	$\mathrm{f(x,y,z) = 4sin(x)cos(y)cos(z) - (cos(x)cos(y) + cos(y)cos(z) + cos(x)cos(z))}$	(2-7)
S8	$\mathrm{f(x,y,z) = 8cos\left(\frac{x}{2}\right) cos\left(\frac{z}{2}\right) sin\left(\frac{x}{2}\right) + 8cos\left(\frac{y}{2}\right) cos\left(\frac{z}{2}\right) sin\left(\frac{y}{2}\right) + 8cos\left(\frac{x}{2}\right) cos\left(\frac{y}{2}\right) sin\left(\frac{z}{2}\right)}$	(2-8)
S9	$\mathrm{f(x,y,z) = sin(x)\,sin(y) + sin(x)\,sin(y) + sin(x)\,sin(y) - 4\,cos(x)\,cos(y)\,cos(z)}$	(2-9)
S10	Stochastic (imposed conditions: vector in z direction, with an average number of 6 ligaments intersecting at the same point and an average distance between them of 3.5 mm)	

For the design of the structures, an implicit approach was used, using the *Ntopology* and *TPMS Designer* software. With their help, it was possible to analyse the printability, the variation of the constructive parameters depending on the relative density, the degree of anisotropy and the mass distribution inside the samples. Representative figures summarizing the elements of this analysis are presented in Fig. 2-2~~Fig. 2-1~~.

Formatted: Font: 12 pt, Not Bold

Formatted: Font: 12 pt, Not Bold

Formatted: Font: 12 pt, Not Bold, Not Italic, Check spelling and grammar

Formatted: Font: 12 pt, Not Bold

Formatted: Font: 12 pt, Not Bold, Not Italic, Check spelling and grammar

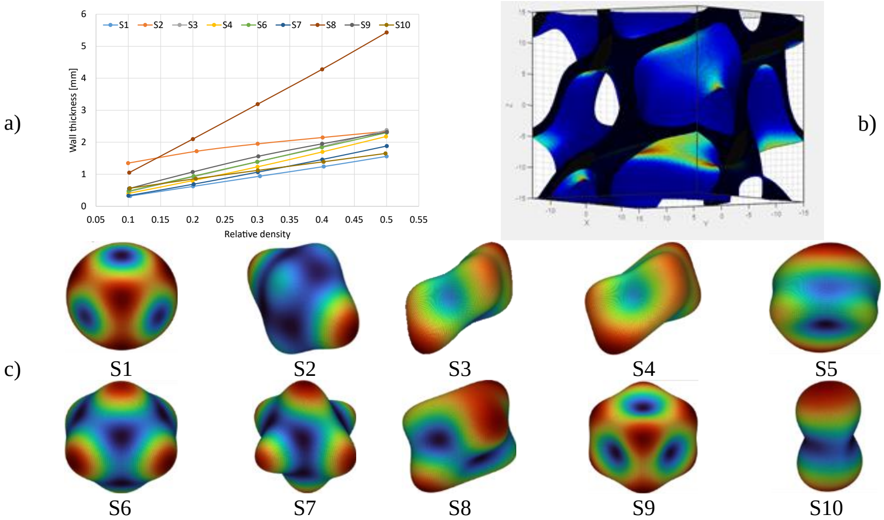

Fig. 2-1 a) Variation of wall thickness depending on the relative density of the samples; b) Representing the need for supports during additive manufacturing; c) Representation of the anisotropy of each sample [26]

Subsequently, an SLA manufacturing technology (Fig. 2-2~~Fig. 2-2~~ a)) was used to print the samples (Fig. 2-2~~Fig. 2-2~~ b)), presenting practical considerations regarding the successful fabrication of such complex geometries. Tensile tests were performed to validate the properties of the photopolymer used. In general, these coincided with the values declared by the manufacturer, except for the specific deformation at break, where significant differences of up to 22% were identified.

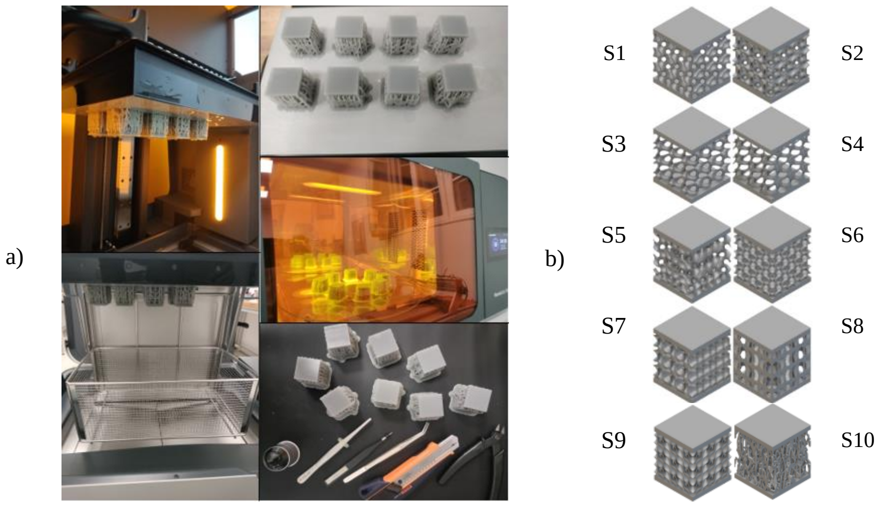

Fig. 2-2 a) Sample fabrication through stereolithography; b) Each type of specimen

Formatted: Font: 12 pt, Not Bold

Formatted: Font: 12 pt, Not Bold, Not Italic, Check spelling and grammar

Formatted: Font: 12 pt, Not Bold

Formatted: Font: 12 pt, Not Bold, Not Italic, Check spelling and grammar

Formatted: Font: 12 pt, Not Bold

Formatted: Font: 12 pt, Not Bold, Not Italic, Check spelling and grammar

Formatted: Font: 12 pt, Not Bold

Formatted: Font: 12 pt, Not Bold, Not Italic, Check spelling and grammar

Next, an analysis of the quality of the manufactured samples was carried out in terms of surface roughness, dimensional and mass deviations and internal porosity of the material.

Following additive manufacturing, a discrepancy was also determined in terms of the density of the resin after polymerization, which had a higher value of 1.23 g/cm^3 than the value declared by the manufacturer of 1.07 g/cm^3. Most likely, this value is specific to the uncured liquid resin, and the difference in density is associated with a more compact molecular structure of the polymerized parts. Such a difference has also been reported in the relevant literature, such as [27,28] or specified by other resin manufacturers [29]. A direct link between the maximum surface area of the topologies and the deviation from the average mass was also determined, which indicates that samples with complex and reduced geometric characteristics must be subjected to intensive washing treatments. This is necessary to successfully remove the entire mass of resin that adhered to the surface of the part before it was cured in the treatment chamber.

By three-dimensional scanning of the manufactured samples, it was determined that there were no significant deviations from the designed CAD geometry, the only dimensions that went out of the imposed tolerance of 0.1 mm being at the level of the lower areas where the part came into contact with the plate supporting the side supports. This can be eliminated by changing the printer settings to impose a greater distance between the components or by completely abandoning the support plate. The dimensional deviations are consistent with those specified in other publications, where the average difference from the nominal values varied between 0.045 mm and 0.15 mm [30] or from 0.042 mm to 0.127 mm [31]. Also, Emir and Ayyildiz specify in [32] that the average dimensional deviations of an SLA technique have a value of 68.5 µm, significantly higher than those indicated in the process used in this work.

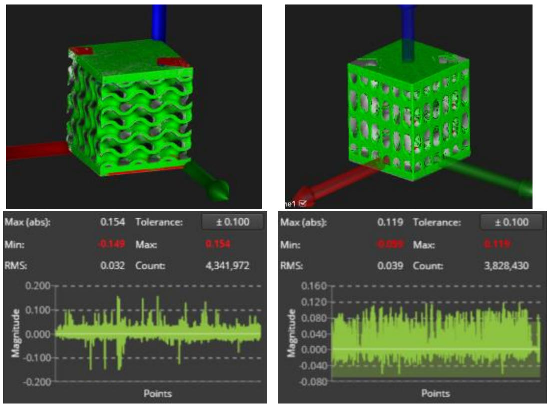

Fig. 2-3 a) Dimensional deviations for S1; b) Dimensional deviations for S8; c) Deviations distribution for S1; d) Deviations distribution for S8

By analysing the roughness of the flat surfaces of the samples, it was determined that, although there were differences between surfaces of the same type, the same surfaces presented very similar roughness, which denotes a stable manufacturing process, without fluctuations. In terms of value, the roughness analysis validated the results previously obtained in the dimensional analysis, with no frequent Rp values above the imposed limit of 0.1 mm. The average roughness Ra was 2.47 µm, a value specific to well-controlled additive manufacturing processes, and the average distance between the highest and lowest points of the profiles was 26.32 µm. These values indicate a very good quality of the surfaces and the lack of layer-by-layer appearance, therefore a good homogeneity of the part, without the need for grinding procedures or additional processing. The values obtained for the roughness Ra are in line with relevant studies on the same topic, such as those specified in [33]: 0.87–4.44 µm, then in [34]: 0.71– 2.91 µm or in [35]: 2.66 - 3.37 µm. However, this aspect can be improved because other works suggest lower values of roughness.

In order to detect defects that are impossible to see with the naked eye, a microscopic analysis of the outer surfaces of the part was performed. Most of the analysed surfaces did not present defects, reinforcing the idea that the chosen manufacturing process is suitable for the designed geometries. Different types of possible superficial defects were highlighted, some of which can be limited by a more careful control of the way in which the resin is stored between successive prints. Also, an important aspect to avoid damage to the parts is the very thorough cleaning of the residual resin, as it is adherent and tends to accumulate impurities. Furthermore, careful handling of the samples before being introduced into the ultraviolet radiation treatment chamber can limit the appearance of surface defects.

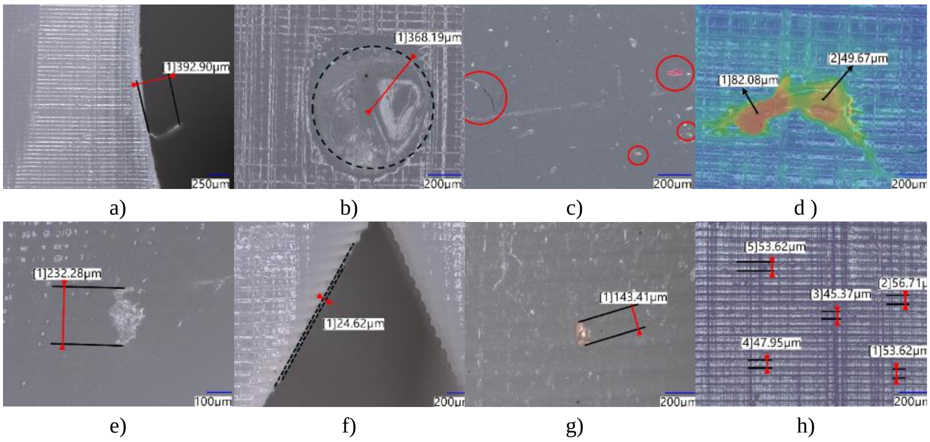

Fig. 2-4 Examples of defects: a) Superficial micro-exfoliation; b) Trace left by removing printing supports; c) Impurities embedded in resin; e) Protuberance on the surface of the part; e) Excess polymerized resin; f) Micro-irregularities; g) Contamination with sand grains; h) Layer-by-layer appearance [36]

To analyse the internal defects of the samples, a non-destructive method of analysis using ultrasonic waves was used. The flat surfaces large enough to allow the probe to contact were checked, there being no indications of the presence of defects in the depth of the samples. This testing method excluded the presence of major defects, such as exfoliations or internal voids, but in order to verify whether there are very small porosities, which cannot be captured by non-destructive methods, it was decided to perform an internal analysis of the samples. The pieces were cut by water jet cutting and the generated surfaces were analysed. By comparison with the lateral surfaces, a better homogeneity was found in the depth of the pieces and a lack of the layer-by-layer appearance, which is still visible on the outside under a microscope. The lack of inclusions of other materials inside the sample may indicate that the incidents of impurities on the outer surface are not a consequence of non-compliant storage, but of inadequate post-processing before hardening. In the multitude of surfaces checked, there were also micro-porosities in the processed surfaces, which may indicate either insufficiently polymerized internal voids that were removed at the time of cutting, or are the consequence of an inadequate cutting process. Whatever the cause, there are indications related to the possibility of the appearance of local inhomogeneities, which could be better identified in a subsequent analysis by subjecting the samples to X-ray checks.

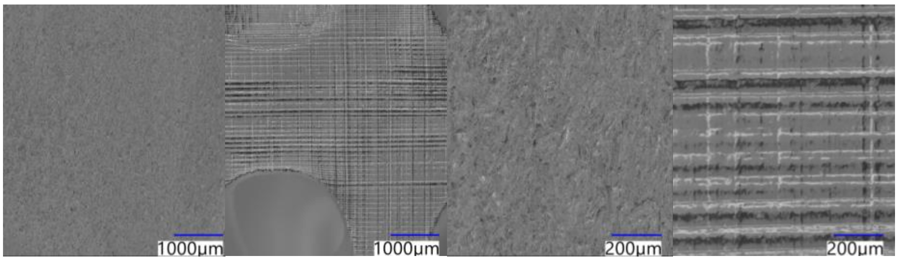

a) b) c) d)

Fig. 2-5 a) Section exposed through cutting, x40; b) Lateral surface, x40; c) Section exposed through cutting, x200; d) Lateral surface, x200

By interpreting the results obtained, a very low standard deviation of the sample mass and roughness values was observed, which denotes a narrow distribution of the parameters and a high reproducibility of the manufacturing technology, without any indications of the existence of significant defects likely to critically influence the behaviour of the analysed samples.

CHAPTER 3 COMPRESSIVE TESTING OF THE PROPOSED METAMATERIAL SAMPLES

Among the defined metamaterial geometries we find the gyroid-type shape S1 extensively studied in the literature, adopted in the work as a comparison standard, other TPMS structures based on thin walls similar to the gyroid (S2, S3, S4, S7, S8, S9), the stochastic structure (S10) that behaved like a metamaterial based on interconnected ligaments, structures with wall thickness variation along the loading direction (S5) and structures with considerably reduced dimensions of the constitutive geometric features (S6).

Following uniaxial compression testing, the proposed cores presented different deformation methods, identified in Fig. 1-1~~Fig. 3-1~~. Topologies S1, S6, S7 and S8 exhibited a "bending-dominated" behaviour, characterized by a long plateau, with negligible material softening and reduced fluctuations in the loading force. The effect is a constant or continuously increasing response of the capable force during deformation. The structures S2, S3, S4, S5 and S9 showed a mixed behaviour, "bending-dominated" and "stretching-dominated", where the yield is followed by a "softening" zone, in which the bearing force decreases with local buckling or wall bending, until the contact between them, which gives rise to a new stiffening stage. Depending on the way the material is arranged inside the sample, the number of steps differs affecting the overall deformation mechanism and the energy absorption capacity. The stochastic structure showed a pure "stretching-dominated" behaviour, where the axial forces in the core ligaments led to rapid buckling after the elastic stop, resulting in a much more pronounced reduction in the bearing capacity and energy absorption. However, compared to the gyroid evolution, the stochastic structure exhibited superior stiffness results in the elastic deformation zone and a force corresponding to the onset of flow higher by approximately 6%. The results thus highlight the differences between the two types of three-dimensional metamaterials mentioned and manage to attribute to each a predefined type of deformation in accordance with research in the literature [37], [38].

Formatted: Font: 12 pt, Not Bold

Formatted: Font: 12 pt, Not Bold, Not Italic, Check spelling and grammar

Formatted: Font: 12 pt, Not Bold

Formatted: Font: 12 pt, Not Bold, Not Italic, Check spelling and grammar

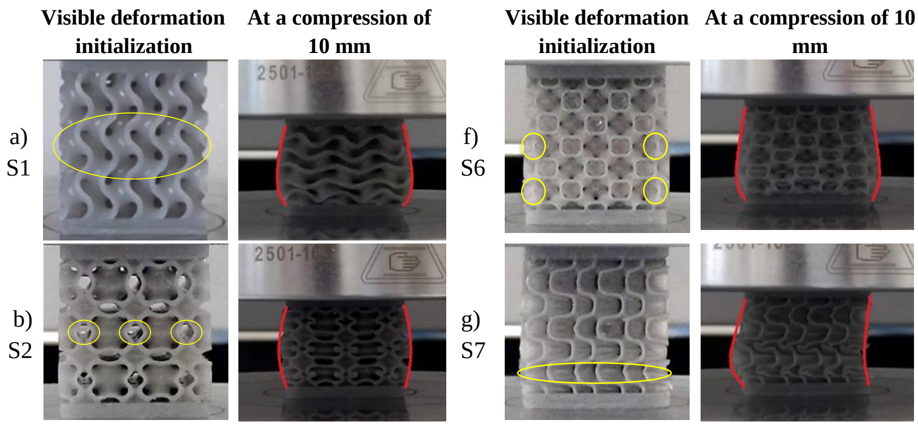

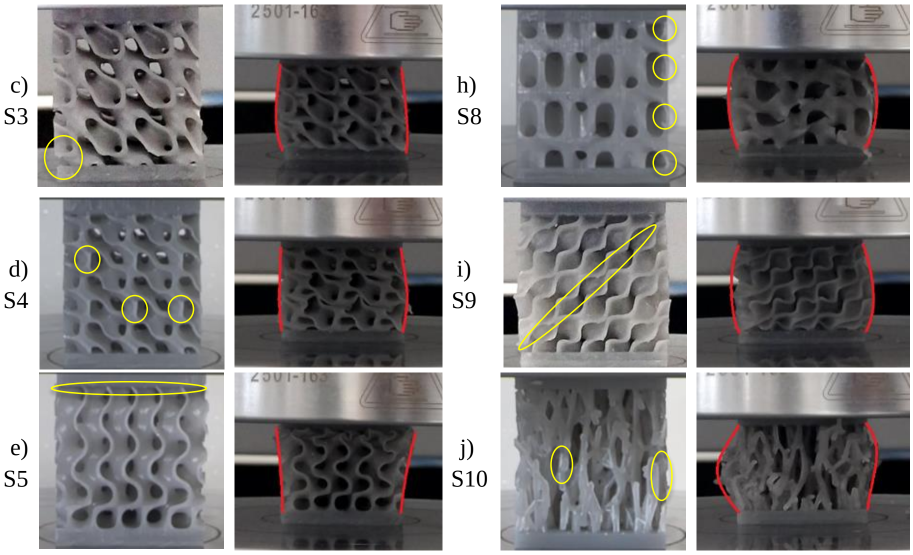

Fig. 1-1 Images from compression testing for each sample at the moment when visible deformation initiation was observed and at a compression of 10 mm [39]

Compared to the gyroid, the S8 topology showed a similar evolution of the load capacity, with significantly higher values of up to 31% of the value of the force corresponding to the yield point and a higher densification rate. The surplus of the capable force suggests that an equivalent geometry, but with a lower relative density, could lead to values similar to those obtained by testing the gyroid-type structure, but with the advantage of reducing mass.

Regarding the energy absorption efficiency, it was highlighted that the structures with higher values are those whose stresses do not show significant fluctuations during the loading, but offer a clear and long yield plateau. Thus, the S8 and S1 samples showed close values, while the curves specific to the other TPMS topologies showed significant reductions in efficiency, given the significant fluctuations of the compressive force. These were maximum in the case of stochastic geometry, which had the lowest efficiency at high values of specific strain.

In order to estimate the mechanical properties at different relative densities, a model specific to structures based on interconnected ligaments with open cells was used. The evolution of the variation of the elastic modulus and the yield stress was presented based on the known values for the relative density chosen in the experiments. It was observed that in most cases, the values are found between the limits mentioned in the literature specific to polymers, except for a single case encountered in specimen S8. This deviation can be based on the differences between the manufacturing technologies and the wide family of materials to which the limits are assigned.

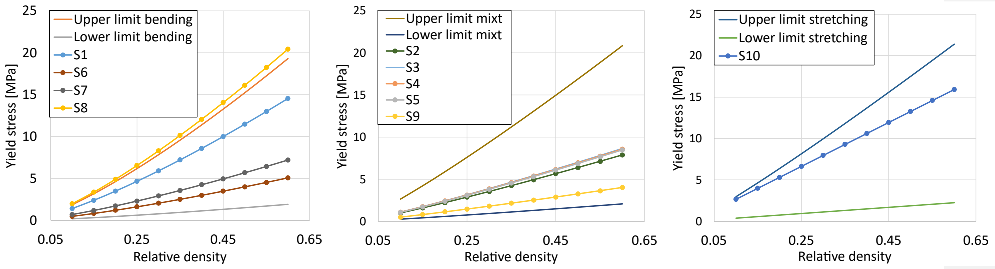

a) b) c)

Fig. 1-2 Variation of yield stress as a function of the relative density of the samples for different behaviours: d) bending; e) mixt; f) stretching

Four ways of modifying the initially proposed uniform geometries were presented (Fig. 1-3~~Fig. 3-3~~). They demonstrate the high capabilities of core customization based on implicit modeling and show how choosing a configuration with a different number or shape of the representative cell influences the mechanical behaviours. It was observed that the use of a lower number of cells provides a higher compressive strength, but also a lower specific strain to the appearance of the first cracks, while the use of a higher number of cells distributes the stress more evenly in the sample mass and allows higher specific strains at the expense of the loading force and stiffness. The use of a wall thickness gradient leads to a localized deformation in the upper zone together with a specific plastic zone plateau and a lower energy absorption than the homogeneous model.

Formatted: Font: 12 pt, Not Bold

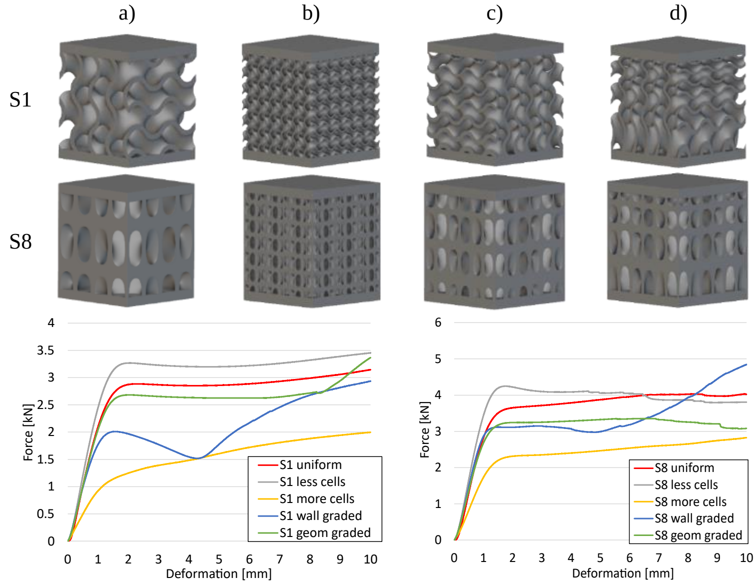

e) f)

Fig. 1-3 Shape changes for S1 and S8: a) 2x2x2; b) 6x6x6; c) Applying a wall thickness gradient; d) Applying a cell height gradient; e) Compressive force versus strain diagram for S1; b) Compressive force versus strain diagram for S8

Analysing the way in which the configurations return to dimensions close to the nominal ones after being subjected to a specific deformation of 33.33%, it was observed that they are suitable for applications where repeated stresses occur. In this regard, cyclic tests were performed, observing the evolution of the energy absorption capacity for each sample. It was observed that for stresses in the elastic domain, S1 ranked third, after S8 and S10, which however had a faster rate of accumulation of residual deformation. Finally, it can be mentioned that the S1 gyroid had a mechanical behaviour slightly inferior to the S8 specimen, while the S10 stochastic geometry had a behaviour specific to metamaterials based on three-dimensional interconnected ligaments, for which the cracks in the depth of the piece determined an inferior behaviour in a repeated test.

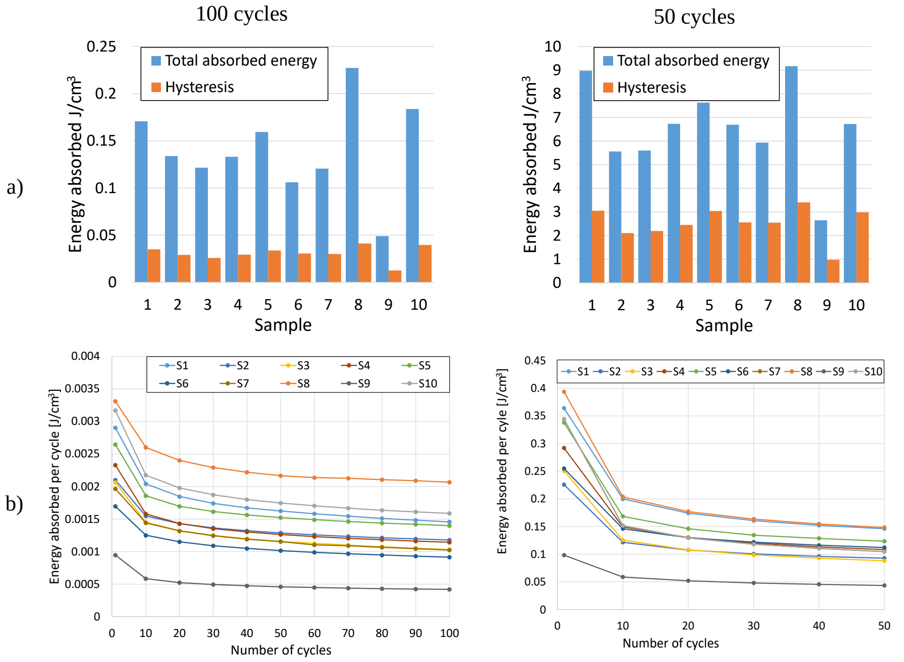

Fig. 1-4 a) Total energy absorbed during loading and hysteresis, during; b) Variation of energy absorbed during 100 /50 cycles [40]

CHAPTER 4 NUMERICAL SIMULATION OF COMPRESSION TESTS

Following a convergence analysis of the discretization, it was established that a maximum size of the side of the regular tetrahedron elements of 0.3 mm provides an optimal balance between the accuracy of the results and the increase in the computational effort required to obtain a solution. The use of a single discretization may, however, prove insufficient in the case of cores with walls whose thickness is not constant or in areas with very low thicknesses, where at least two rows of elements cannot be built, resulting in convergence problems or reductions in accuracy, such as the case of the S4 and S10 configurations.

An analysis of the implications of the use of implicit modelling in finite element simulation was performed. For the same gyroid topology, geometric models obtained both by the conventional CAD method (Fig. 2-1Fig. 4-1a)) and by a proprietary method, which allows the integration of the geometries obtained by implicit modelling into numerical analyses (Fig. 2-1Fig. 4-1b)). The dimensional deviations exceeded the imposed tolerance value of 0.1 mm, with maximum values of 0.17 mm. However, the results obtained regarding the curves of variation of the compressive force as a function of deformation (Fig. 2-1Fig. 4-1c)) showed a very good overlap between the two models. A disadvantage is the fact that for the use of a geometry obtained by implicit modelling, the times required to establish the faceted geometry, transform the geometry into a solid, discretize and obtain the solution are significantly higher. They can be up to five times higher than in the case of a conventional approach, which makes the finer discretization of solids even more difficult due to the rapid increase in the computational effort.

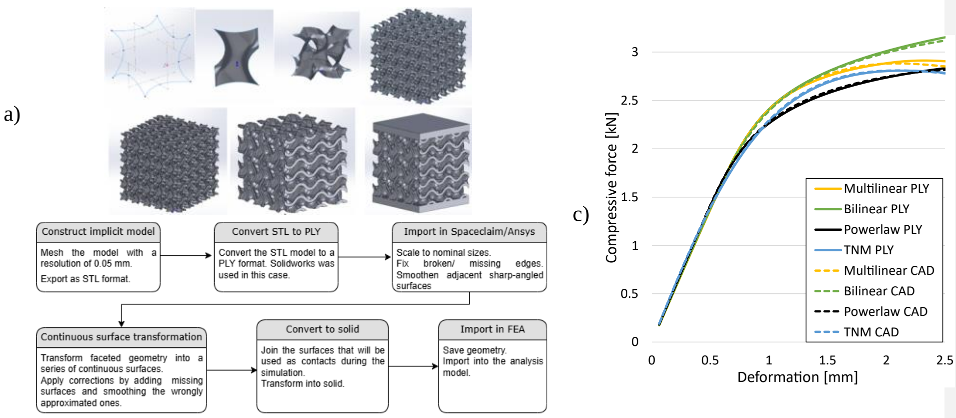

Fig. 2-1 a) Creating the CAD geometry of sample S1; b) Procedure for obtaining solids usable in finite model analysis starting from implicit modelling; c) Evolution of the loading force of sample S1 depending on the type of geometry used

Four material models were proposed (Fig. 2-2Fig. 4-2 a)-d)) and it was verified which of them most closely approximates the behaviour of the chosen photopolymer resin. With the help of the data obtained experimentally through tensile tests, two isotropic material models were empirically defined, the bilinear and the multilinear. Next, an iterative method was used to configure two other material models, *Powerlaw* and *Three Network Model*. The parameters defining their equations were configured so that the characteristic curves of the material behaviour overlap as accurately as possible over the real average characteristic curve and

Formatted: Font: 12 pt, Not Bold
Formatted: Font: 12 pt, Not Bold, Not Italic, Check spelling and grammar
Formatted: Font: 12 pt, Not Bold
Formatted: Font: 12 pt, Not Bold, Not Italic, Check spelling and grammar
Formatted: Font: 12 pt, Not Bold
Formatted: Font: 12 pt, Not Bold, Not Italic, Check spelling and grammar
Formatted: Font: 12 pt, Not Bold
Formatted: Font: 12 pt, Not Bold, Not Italic, Check spelling and grammar
Formatted: Font: 12 pt, Not Bold
Formatted: Font: 12 pt, Not Bold, Not Italic, Check spelling and grammar
Formatted: Font: 12 pt, Not Bold
Formatted: Font: 12 pt, Not Bold, Not Italic, Check spelling and grammar
Formatted: Font: 12 pt, Not Bold
Formatted: Font: 12 pt, Not Bold, Not Italic, Check spelling and grammar
Formatted: Font: 12 pt, Not Bold
Formatted: Font: 12 pt, Not Bold, Not Italic, Check spelling and grammar

presented so that the material model is easy to replicate in the Ansys calculation program. Following the tests carried out on the four types of materials, it was verified how large the deviation of each one is from the experimentally determined average force-strain curve (Fig. 2-2Fig. 4-2 e)). Deviations of less than 6% were found, the optimal model being the multilinear one which had a deviation of only 2.54%.

Formatted: Font: 12 pt, Not Bold

Formatted: Font: 12 pt, Not Bold, Not Italic, Check spelling and grammar

Formatted: Font: 12 pt, Not Bold

Formatted: Font: 12 pt, Not Bold, Not Italic, Check spelling and grammar

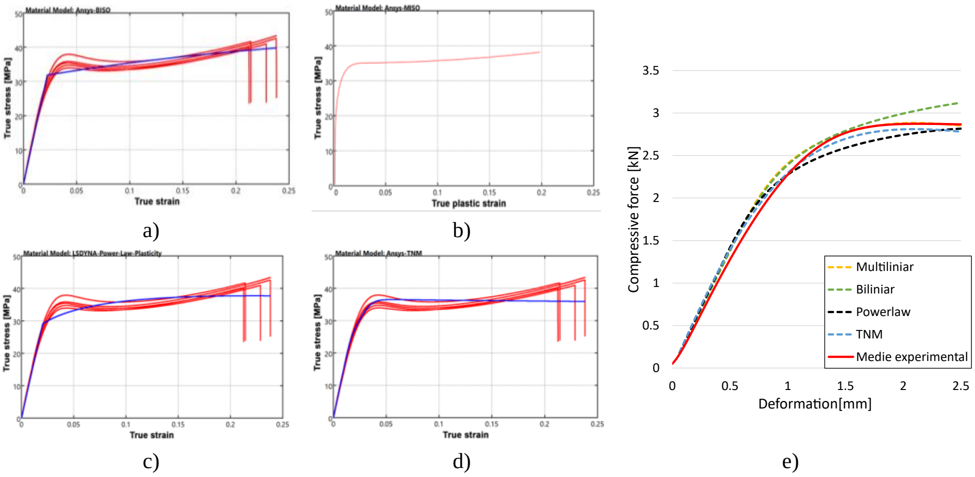

Fig. 2-2 a) *Bilinear isotropic hardening* model; b) *Multilinear isotropic hardening* model; c) *Power Law Plasticity* model; d) *Three Network Model*; e) Evolution of the loading force of the S1 specimen as a function of deformation for the defined material models

Two types of finite element simulations were performed, the one performed in the *NTopology* software and the one performed in Ansys Static Structural. Studying the difference between the two analyses, it can be seen that in terms of the distribution of the von Mises equivalent stresses there is a high degree of similarity. The limitations of the material definition mode in *NTopology* make the differences between the maximum equivalent stress values substantial, even greater than 100% as is the case for samples S1 and S10. In addition, the simulations in the Ansys module provide clearer indications leading to the anticipation of the deformation mode of samples such as those of topologies S2, S7 and S9. However, as a first step in a rapid prototyping effort, the simulation module in *NTopology* can provide a sufficiently accurate answer for faster filtering of topologies according to the desired mechanical response.

Performing quasi-static numerical analyses that include large deformations on complex three-dimensional geometries can prove difficult due to the contacts that occur inside the samples. Increasing the tolerance of the walls penetrating each other can increase the convergence rate but will also lead to reduced accuracies. In this sense, static tests were performed on a deformation of only 2.5mm, a value chosen so that no contacts occur that would lead to difficulties in obtaining a solution. Even in this case, due to the periodic nature that determined thin walls on the contour of the S4 core, the deformation value was reduced to 1mm so that the simulation converges to a solution, even if a smaller area of the flow phenomenon is captured. Avoiding or minimizing these situations can be done by modifying the range of the function that defines the part or by subsequent rotation of the representative cell around an axis. It should be borne in mind that the latter would lead to other types of mechanical behaviours, since the geometries are not symmetrical in both directions

By corroborating the field of von Mises equivalent stresses and total equivalent strains obtained for each sample, conclusions can be drawn regarding the general failure mode of the samples. In general, all these conclusions lead to a deformation mechanism similar to that identified by experimental tests. Sample S6 is the exception to the rule, the more significant deformation in the lower area not being able to be identified by simulation. There is a possibility that its failure mode is influenced by manufacturing defects that have not been previously identified, especially considering the topology of the representative cell with smaller dimensions than the other samples.

Analysing the force-strain compression curves obtained by simulation and comparing them with the experimental ones (Fig. 4-3Fig. 4-3) it can be observed that the overlap is optimal only for samples S1 and S8 that presented the highest values of the yield strength. The other samples show significant deviations as its value decreases. However, the shape of the curve is maintained, and a more accurate characterization of the material used can lead to significant improvement of the results, especially in the plastic limit area. The nonlinear nature of the behaviour of polymers makes it difficult to accurately simulate the reality of experimental determinations due to high deformations that lead to discretization distortions and convergence problems. In addition, the transition to plastic behaviour is much more sensitive and complex than in the case of conventional materials. Also, the contacts that inevitably occur inside complex TPMS-type geometries introduce additional nonlinearities because the boundary conditions change as the deformed surfaces come into contact.

Formatted: Font: 12 pt, Not Bold

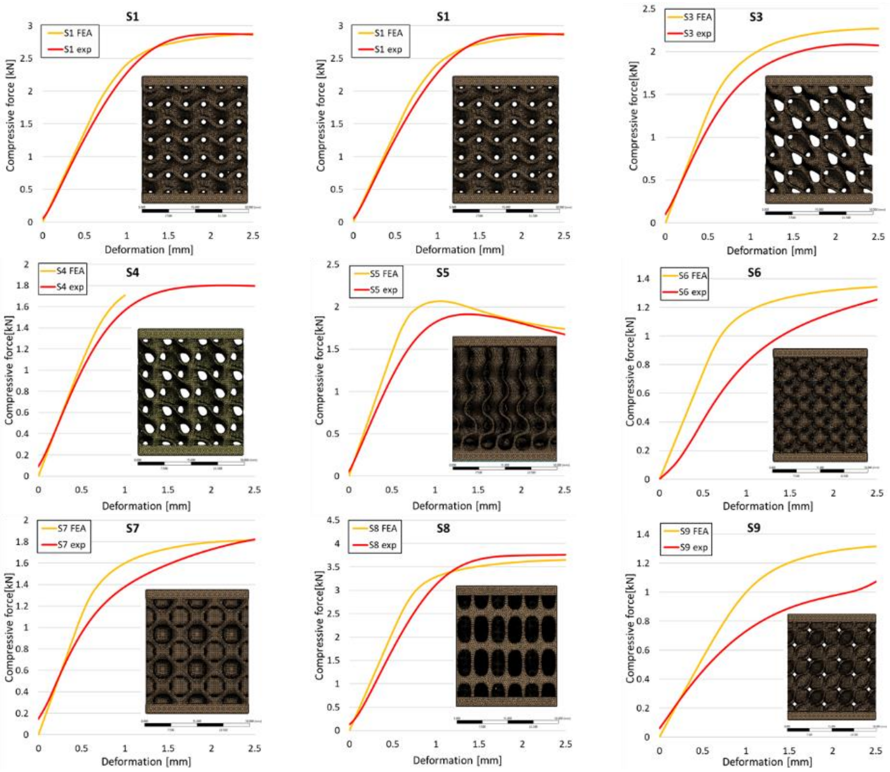

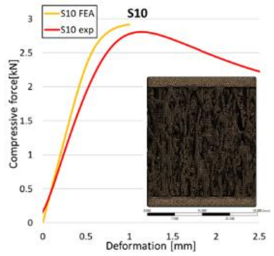

Fig. 4-3 Comparison between the force-strain curves obtained experimentally and by finite element analysis for each geometry [41]

The analysis in the *Explicit Dynamics* module captured the overlapping of the cell layers more accurately, leading to similar results in the low-strain zone. However, it showed a noticeable reduction in the material loading force at high strain values, which is based on the nonlinearity of the material. Thus, this calculation model also fails to perfectly capture the phenomenon of gradual stiffening of the proposed cores. However, in the case of this analysis as well as in the case of the static analysis, the failure mode coincided with the one identified experimentally.

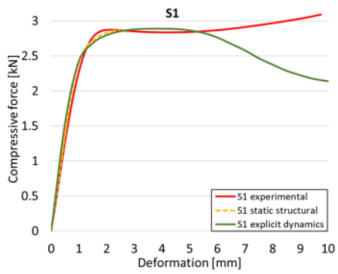

a)

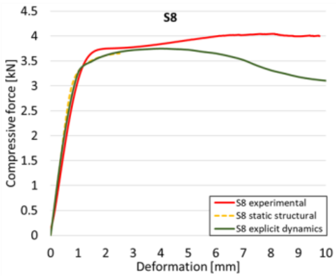

b)

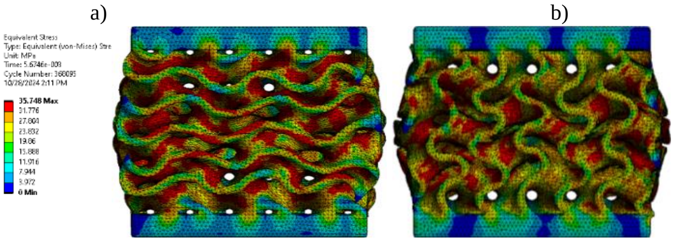

c) S1

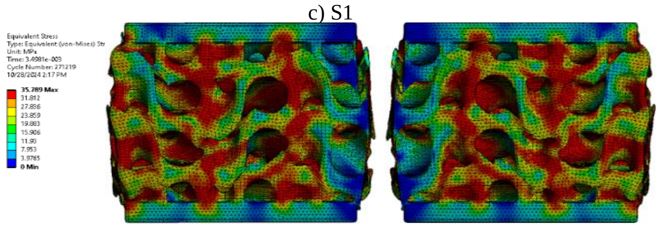

d) S8

Fig. 2-4 Comparison between the real force-strain curve and those obtained by finite element analysis for: a) S1; b) S8; The von Mises equivalent stress field in two views, front and side, for: c) S1; d) S8;

CHAPTER 5 LOW SPEED IMPACT TESTING

The chapter aims to extend the understanding of the behaviour of TPMS and stochastic structures proposed in the previous chapters, through low-velocity impact tests. The two most promising types of triple periodic topologies and stochastic topology were chosen. As an extension of the study and due to the interest in this direction in the specialized literature, it was proposed to fill the gaps in the TPMS cores with a two-component silicone solution, vulcanized at room temperature (RTV). The topology of the proposed cores makes such an approach possible, due to the fact that one or more continuously communicating volumes are generated inside that can be filled with filler material, without having closed enclosures.

10 samples of the same material used previously were proposed and made by stereolithography (SLA) to be tested for impact at two different energies. For filling with filler material, the specific recommendations for the silicone type material are adopted for its homogenization, then a proprietary method is proposed to ensure the elimination of as much as possible of the silicone porosity inside the printed samples (Fig. 1-1~~Fig. 5-1~~). From our own observations, the use of a vacuum pump is insufficient to achieve a homogeneous structure. The process used thus involves mixing the solution and using the vacuum pump to extract the air incorporated during mixing. Then, it is poured into the moulds made for easy subsequent extraction, and the enclosure is mounted on an exciter to introduce vibrations in the vertical direction and is again connected to the vacuum pump for another 8-10 minutes. After 24 hours, the parts are extracted from the moulds and the excess material is removed.

Formatted: Font: 12 pt, Not Bold, Not Italic, Font color: Auto

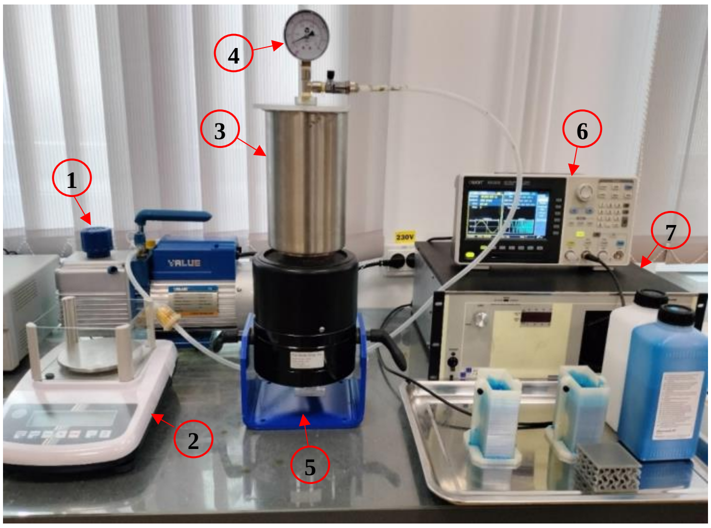

1. Vacuum pump VE2100N
2. Precision balance PFB2000-2
3. Vacuum chamber
4. Pressure gauge
5. Shaker 2075E
6. Arbitrary function generator XDG2035
7. Power amplifier 2050E09

Formatted: Left

Fig. 1-1 Installation for removing air from the sample volume

The obtained samples were tested at low-velocity impacts, with energies of 30 J and 40 J. To allow for comparison of the performances of the proposed structures, the parameters presented in Table 1-1~~Table 5-1~~ were evaluated. The highest and lowest values of the parameters were highlighted in green and red, respectively, for each set of tests.

Formatted: Font: 12 pt, Not Bold

Table 1-1 Parameters for evaluating the performance of structures under impact loads

Sample type	Impact energy	Mass	Maximum force	Maximum deformation	Total absorbed energy	Average force	Specific absorbed energy	Impact force efficiency	Recovered energy	Damping index
	[J]	[g]	[kN]	[mm]	[J]	[kN]	[J/kg]	[-]	[J]	[-]
S1_1	30	67	5,413	7,76	29,07	3,75	433,95	0,692	0,93	31,25
S1_2	30	147	6,35	7,33	29,72	4,05	201,90	0,639	0,28	106,14
S8_1	30	66,6	5,798	8,33	29,78	3,58	447,08	0,617	0,22	135,36
S8_2	30	146	7,911	10,43	29,88	2,86	204,24	0,362	0,12	249
S10_1	30	67,8	3,275	17,27	30,19	1,75	445,48	0,534	0,19	158,89
S1_3	40	66,1	4,428	15,09	40,35	2,67	610,72	0,604	0,35	115,28
S1_4	40	147	7,067	7,86	37,17	4,73	253,72	0,669	2,83	13,13
S8_3	40	66	8,869	12,81	39,75	3,10	602,18	0,350	0,25	159
S8_4	40	147	6,271	13,04	39,61	3,04	268.,91	0,484	0,39	101,56
S10_2	40	66,3	4,526	13,82	39,93	2,89	601,90	0,638	0,07	570,42

A first observation is that the manufacturing process remains optimal, due to the minimal deviations that occur between the masses of specimens of the same type. The standard deviation for samples without filler material was 0.66 while for those with the addition of silicone it was 0.49. However, filling the sandwich specimens leads to obtaining structures with a final mass 2.2 times (219%) higher than the initial ones, which may present an impediment in situations where mass is an important criterion.

Fig. 1-2Fig. 5-2 shows the evolution of the impact force as a function of the impactor displacement for S1, S8 and S10, with and without silicone. Studying the value of the maximum force obtained, it is observed that the use of silicone filler led, in three out of four cases, to stiffer samples, which develop higher impact response forces. However, the maximum force is recorded for the simple S8 structure, tested at an impact energy of 40 J, in which case the addition of silicone resulted in a lower force value. Due to the unexpected response, another test was performed to study the repeatability of the data, which validated the response obtained. Another observation is that the S8 structure presents higher impact force values compared to the classic gyroid, while the sample with stochastic core obtained the lowest values during both tests, due to the reduced stiffness of the ligaments used.

Formatted: Font: 12 pt, Not Bold

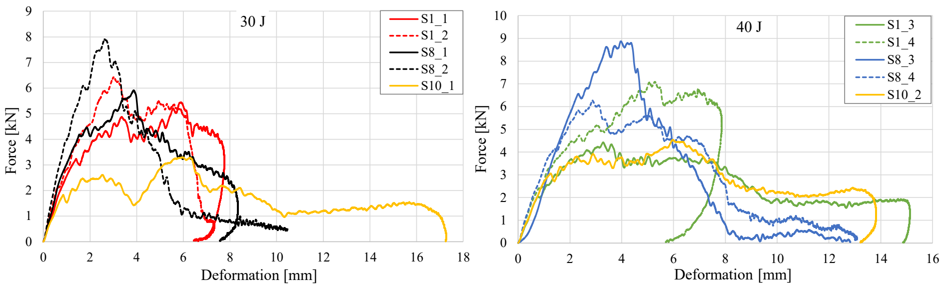

a) b)

Fig. 1-2 Evolution of impact force as a function of displacement for: a) 30 J; b) 40 J

Most of the time, a high impact force was also accompanied by a high value of the impactor displacement and implicitly of the sample indentation. This is the case for structures

S1_2, S8_2, S8_3, S8_4, for which the cracking of the upper face also caused the core to break along the entire height. So, although the S8 topology presents higher values of the maximum impact force, it is more susceptible to the loss of structural integrity, especially at high values of the impact energy. In contrast, samples S1_1, S8_1 and S1_4 presented only damage to the upper face, with minimal cracking in the depth of the core. Structures S10_1 and S10_2 allowed high local deformations, and the impactor destroyed the ligaments in the impact area, without generating total destruction of the pieces. This phenomenon is most visible in the stochastic topology, but was also encountered in the 40 J energy test on the gyroid sample, S1_3.

During the tests, all samples reached the imposed threshold of 30 J and 40 J, respectively. However, some of them absorbed this energy in full, and others transmitted a small part of it back to the impactor. The absorbed energy is controlled by the plastic damage of the samples, so the sample with the best absorption capacity is sample S1_3, which deformed up to a value of 15 mm, while the sample that absorbed the least part of the impact energy introduced during the tests was S1_4, whose resistance led to the transmission back to the impactor of a higher energy, 2.83 J. It can be concluded that a structure with a low value of the energy reintroduced into the system at the end of the test, presented in the penultimate column of Table 1-1~~Table 5-2~~, is favourable in energy absorption applications, since it can lead to the reduction of the damage caused to the object impacting the sample. On the other hand, if it is desired that the struck object suffers as little damage as possible, it is desirable that the recovered energy have higher values, as is the case with gyroid-type samples.

Although the S8 topology presented in most cases higher values of the impact force, the significant deformations make the average impact force have the highest value in the case of the S1_4 sample, due to the lack of plastic deformation and impactor rebound. At the opposite pole are the pieces with stochastic core that presented the most significant deformations, resulting in a reduced average impact force. If the additional mass introduced by the silicone filler is taken into account, it is observed that the hybrid structures lead to much lower specific absorbed energy values. Values up to 215% lower were obtained following tests with an impact energy of 30 J, respectively 240% for 40 J.

The existence of significant oscillations in the impact force values is highlighted by the impact force efficiency. The narrower its evolution distribution, the more it is considered that the structure can absorb the impact energy more efficiently, without introducing large stress gradients during the phenomenon, which can cause significant plastic deformations. In this case, structures with gyroid and stochastic cores are found, which present efficiencies of 0.6-0.7.

The damping index indicates the system's ability to reduce vibrations after the impact. The lower this index has values; the more structures tend to generate greater vibrations and impactor rebound phenomena. Similarly, structures with high values of the damping index can dissipate more energy and attenuate vibrations more quickly [42]. In most cases, almost all the absorbed energy was used to penetrate the samples and only a small amount of energy was transferred back to the impactor, so the damping is very high. The exceptions are the structures S1_1 and S1_4.

Taking all this into account, it can be concluded that sandwich structures with TPMS and stochastic cores are optimal solutions for applications where energy absorption is important. The S8 structure showed higher performance at lower impact energy values, but it plastically deformed faster by losing structural integrity at higher energies. At the same time, the stochastic structure showed the most predictable response, localizing the deformation, without endangering the integrity of the panel, in accordance with similar observations in the literature [43].

Regarding the use of silicone filler material, the solution generally leads to a stiffer response from the structures, as a result of testing at high impact energies, but does not

Formatted: Font: 12 pt, Not Bold

Formatted: Font: 12 pt, Not Bold, Not Italic, Check spelling and grammar

Formatted: Font: 12 pt, Not Bold

Formatted: Font: 12 pt, Not Bold, Not Italic, Check spelling and grammar

significantly improve the energy absorption properties. Given the process of obtaining such homogeneous structures, especially on a large scale, as well as the additional mass they imply, their use is effective only in specific applications, where it is desired to prevent the destruction of the panels, the silicone acting as a binder between the chambers generated in the core volume. The proposal to use the filling made with bi-component silicone is, however, only an example used to illustrate the hybrid design concept that can be used for a TPMS type geometry and its manufacturing feasibility. The proposed structures can find applicability in different fields, such as vibration damping, impact mitigation systems or other specific applications.

CHAPTER 6 FINAL CONCLUSIONS

1.1 General conclusions

The doctoral thesis presents experimental and numerical analyses of the low-velocity compression and impact behaviour of innovative sandwich configurations with mechanical metamaterial cores. Based on the study, the following general observations and conclusions can be drawn:

- Eight new TPMS configurations and a stochastic geometry were developed, with the aim of comparing their mechanical performance with that of a gyroid structure, often found in the literature. Thus, the capabilities of implicit modelling to generate novel metamaterial topologies were demonstrated.
- There are software programs that allow the development of a method by which such topologies can be defined and analysed in terms of manufacturing possibilities, anisotropy degree or constructive parameters.
- Implicit modelling allows for rapid scaling and modification of constructive parameters. This was demonstrated by altering the basic topology in four different ways, using techniques that cannot be implemented by conventional computational design. 19 types of specimens, of different geometries or dimensions, were thus designed.
- It has been proven that the SLA manufacturing technique can print TPMS and stochastic topologies with representative cell sizes up to 5 mm and wall thicknesses up to 0.3 mm. The adopted settings that generated specimens of optimal quality are based on the following observations and recommendations:
    - avoiding the generation of closed enclosures in the volume of the parts, because resin remains embedded in them, which generates significant deviations from the nominal geometry;
    - using a layer thickness of 0.05 mm;
    - printing directly on the printing table;
    - using only side supports whose base is separated from the sample;
    - positioning the samples at a distance from each other on the printing table in order to be able to effectively wash the residual resin deposited on them;
    - upon completion of the manufacturing procedure, it is necessary to minimize the time until the start of post-processing in order to avoid the occurrence of shape deviations;
    - preheating the post-processing enclosure with ultraviolet radiation to guarantee the repeatability of the process on different samples;
    - careful control of the exposure of the resin to ultraviolet radiation and its contamination with impurities.
- The applicability of the chosen manufacturing process was demonstrated by verifying the quality of the parts with the following results:
    - the dimensional deviations of two samples obtained by three-dimensional laser scanning have a root mean square of 35 µm;
    - the average deviation of the sample masses is 1.54% compared to their average value;
    - the average roughness was 2.47 µm, in accordance with the values specified as optimal in the specialized literature;

    - the presence of different types of surface defects that do not endanger the integrity of the samples;
    - the ultrasonic analysis did not identify inhomogeneities in the volume of the parts;
    - the cross-sections of the samples showed optimal homogeneity following a microscopic analysis.
- Quasi-static compression tests were performed for the 10 proposed configurations, each of which was assigned a general deformation mechanism. S1, S6, S7 and S8 exhibited a „bending-dominated” behaviour, characterized by a negligible reduction in the yield strength after the yield zone and a slow densification. S2, S3, S4, S5 and S9 exhibited a “mixed” response, in which the mode of contact of the cell walls determined a stepwise evolution of the compressive force. S10 showed a „stretching-dominated” behaviour, highlighted by the significant reduction in the force value given by the premature rupture of the ligaments. The S8 topology exhibited a force value corresponding to the onset of yielding up to 31% higher, and S10 up to 6% higher, compared to the gyroid geometry.
- Following cyclic compression tests, it was determined that the S8 structure has better energy absorption performance, 39% higher than the S1 sample, in 100 loading cycles in the elastic zone. In the case of cyclic stresses in the plastic deformation zone, S8 remains the configuration with the best results, obtaining only 3% more energy absorbed compared to the gyroid.
- By making changes to the initial geometry, the following were found:
    - a smaller number of cells provides greater compressive strength, but reduces the specific deformation until the first cracks appear;
    - a larger number of cells distributes the stress more evenly in the volume of the part, allowing greater specific deformations, at the expense of the maximum load force and stiffness;
    - applying a gradient of wall thickness determines a localized deformation in the upper area (with the smaller thickness) and a lower energy absorption capacity compared to the homogeneous model;
    - applying a geometric gradient lead to a curve of compressive force as a function of deformation that follows the pattern identified in the case of the uniform sample, but with slightly lower force values.
- Finite element simulation of the quasi-static compression test highlighted the following:
    - a discretization with a maximum size of 0.3 mm or 3 regular tetrahedral elements on the wall thickness ensures an optimal balance between the accuracy of the results and the increase in computing power requirements;
    - the use of geometries obtained by implicit modelling in simulation models does not induce significant errors in the results, but they assume times up to five times longer for the convergence of the results;
    - the four proposed material models approximate the real phenomenon well enough; the multilinear model presented the smallest deviation from the experimental data, with a value of only 2.54% for the gyroid topology S1;
    - using the criterion of von Mises equivalent stresses and total equivalent strains, the failure mechanism of the proposed structures can be

estimated; in eight out of nine TPMS structures, the areas with maximum stress values were the ones that failed first during the experimental tests, leading to a deformation mode similar to the one determined phenomenologically.

- A proprietary method was developed to minimize the porosity of the silicone added as a filler material in the proposed specimens; this involves the use of a two-stage vacuum pump, in parallel with the use of an exciter, which introduces vibrations that facilitate the elimination of air voids from the volume of the part.
- Following the impact tests at low speeds, with energies of 30 J and 40 J, the following were highlighted:
  - in 75% of cases, filling the inner enclosures of the studied topologies with silicone led to the achievement of stiffer sandwich structures, capable of generating impact forces up to 60% higher than in the case of simple, unfilled constructive solutions;
  - the S8 sample generates higher impact forces compared to the gyroid, while the S10 stochastic core configuration recorded the lowest values for both test energies, due to the low stiffness of the ligaments;
  - the S8 sample is more prone to the loss of structural integrity, presenting deformations that are transmitted more easily into the volume of the part, compared to the gyroid topology; the stochastically impacted specimen led to the most predictable results regarding the deformation, which remained localized in the area near the impactor;
  - the additional mass added by the silicone filling obviously leads to hybrid structures with higher mass, but also to significantly lower specific energy absorbed values, up to 215% for an impact energy of 30 J and up to 240% for 40 J.
  - taking into account the impact force efficiency, which implies a higher average impact force and fewer voltage fluctuations during impact, the S1 and S10 structures offer superior efficiencies to the S8 geometry, with values up to 0.6-0.7;
  - the S8 and S10 topologies have a higher damping index than the S1 gyroid topology, making them more suitable for applications where the integrity of the striking object is desired or for vibration damping; on the other hand, the S1 sample was the one that transferred the largest amount of energy back to the impactor, being suitable for applications where the protection of the parts being struck is desired;
  - The use of silicone addition causes a stiffer response of the structures but does not significantly improve the energy absorption performance; taking into account the complexity of the process of obtaining such structures, especially on a large scale, as well as the addition of additional mass, their use is recommended only in specific applications, where preventing the destruction of the sandwich panels is essential, the silicone acting as a binder between the chambers in the core volume.

1.2 Personal contributions

Personal contributions to experimental and numerical methods applicable to the development of metamaterial cores used for sandwich structural components are notable for:

- Design of eight novel TPMS-type topologies and a stochastic geometry, in order to compare the mechanical properties with those of the gyroid (reference configuration in the literature) - Subchapter 2.2
- Construction in the *nTopology* program of a working methodology with clearly defined stages, in order to quickly modify the defining parameters of the created topologies. This also allows imposing a relative density, studying some constructive parameters, verifying anisotropy properties and performing a preliminary numerical simulation - Subchapter 2.3.
- Optimization of the manufacturing parameters of an SLA-type technology, so that over 40 structures with different geometries and dimensions can be printed, with a very high degree of repeatability of the sample quality - Subchapter 2.4.
- Successful use of non-destructive and destructive inspection equipment for parts, rapid prototyping by photopolymerization and those used for the successful addition of filler material in TPMS-type geometries - Subchapters 2.4, 2.5 and 5.2
- Building a procedure through which the quality of parts made by additive manufacturing can be analysed. This includes the determination of dimensional deviations, roughness and surface defects and homogeneity - Subchapter 2.5.
- Performing an experimental and numerical analysis of the behaviour of the 10 proposed topologies under quasi-static and cyclic compressive loads, to determine the structural and energy absorption performances - Subchapter 3.3 and 4.6.
- Studying the implications of altering the basic geometry (changing the cell dimensions and using gradients) on the mechanical response of the samples - Subchapter 3.5.
- Development of a clear methodology for the successful use of geometries obtained by implicit modelling in finite element analyses and presentation of their implications - Subchapter 4.2.2 and 4.6.3.
- Proposing a simplifying method for adapting some material models used in finite element analysis, based on experimental data obtained on the resin used to manufacture the specimens - Subchapter 4.3 and 4.6.2.
- Development of a facility and a method for filling the voids in the volume of TPMS type topologies with liquid vulcanizable rubber material, in order to obtain hybrid specimens with optimal homogeneity - Subchapter 5.2.
- Complementing the experimental analysis in compression with a study of the response of the specimens to impact loads at low speeds, at different impact energies. These were carried out on three types of topologies, both simple and filled with silicone - Subchapter 5.4.

1.3 Future research

- Analysis of defects and homogeneity of samples manufactured by SLA, through imaging techniques such as computed tomography and comparison of the results with those identified by the techniques presented in the paper.
- Study of the mechanical response of the proposed samples to other types of stresses, such as three-point bending or impact at speeds considerably different from those used in the paper.
- Manufacturing of the proposed samples through an additive manufacturing technology based on metal powder sintering and resuming the methodology

from the paper in order to analyse the manufacturing quality and mechanical properties of the samples obtained. It can thus be determined which of the technologies is optimal for printing complex three-dimensional configurations and how these technologies influence the general mechanical behaviour of the structures under the same stresses.

- Making samples from a different type of polymer resin and studying the impact that the material has on the deformation mechanisms. It is intended to determine whether the critical influence on mechanical performance is given by the cell architecture or by the material from which they are manufactured.
- Development of a method to automatically generate new metamaterial topologies, imposing manufacturing and general appearance constraints, filtering them by simulating the mechanical behaviour, either by using the capabilities of the *nTopology* software or by an integrated Python-Ansys approach.

BIBLIOGRAPHY

[1] R. S. Kshetrimayum, “A brief intro to metamaterials,” *IEEE Potentials*, vol. 23, no. 5, pp. 44–46, Dec. 2004, doi: 10.1109/mp.2005.1368916.

[2] Y. Feng, H. Qiu, Y. Gao, H. Zheng, J. Tan, “Creative design for sandwich structures: A review,” *International Journal of Advanced Robotic Systems*, vol. 17, no. 3, May 2020, doi: 10.1177/1729881420921327.

[3] C. Lu, M. Hsieh, Z. Huang, C. Zhang, Y. Lin, Q. Shen, F. Chen, L. Zhang, “Architectural design and additive manufacturing of mechanical metamaterials: A review,” *Engineering*, vol. 17, pp. 44–63, Oct. 2022, doi: 10.1016/j.eng.2021.12.023.

[4] X. Yu, J. Zhou, H. Liang, Z. Jiang, L. Wu, “Mechanical metamaterials associated with stiffness, rigidity and compressibility: A brief review,” *Progress in Materials Science*, vol. 94, pp. 114–173, May 2018, doi: 10.1016/j.pmatsci.2017.12.003.

[5] A. Ronca, G. G. Buonocore, G. Rollo, P. Cerruti, G. Fei, X. Gan, L. Ambrosio, M. Lavorgna, H. Xia, C. Silvestre, “Selective laser sintering fabricated thermoplastic polyurethane/graphene cellular structures with tailorable properties and high strain sensitivity,” *Applied Sciences* 2019, vol. 9, no. 5, 864, Feb. 2019, doi: 10.3390/app9050864.

[6] T. Gao, K. Liu, X. Wang, K. Wei, Z. Wang, “Multi-level mechanism of biomimetic TPMS hybridizations with tailorable global homogeneity and heterogeneity,” *Extreme Mechanics Letters*, vol. 68, 102136, May 2024, doi: 10.1016/j.eml.2024.102136.

[7] Y. P. Wei, H. Li, J. Han, Y. Ma, H. Zhou, J. Cheng, J. Shi, B. Yu, F. Lin, Z. Miao, “Mechanical and damping performances of TPMS lattice metamaterials fabricated by laser powder bed fusion,” *China Foundry*, vol. 21, no. 4, pp. 327–333, Jul. 2024, doi: 10.1007/s41230-024-4026-5/metrics.

[8] C. Yang, W. Wu, Z. Fu, H. Zheng, “Preparation and thermal insulation properties of TPMS 3Y-TZP ceramics using DLP 3D printing technology,” *Journal of Materials Science*, vol. 58, no. 29, pp. 11992–12007, Aug. 2023, doi: 10.1007/s10853-023-08749-0.

[9] N. Novak, M. Borovinšek, O. Al-Ketan, Z. Ren, M. Vesenjak, “Impact and blast resistance of uniform and graded sandwich panels with TPMS cellular structures,” *Composite Structures*, vol. 300, 116174, Nov. 2022, doi: 10.1016/j.compstruct.2022.116174.

[10] J. Song, M. Wang, D. Li, J. Zhang, “Deformation and energy absorption performance of functionally graded TPMS structures fabricated by selective laser melting,” *Applied Sciences*, vol. 14, no. 5, 2064, Mar. 2024, doi: 10.3390/app14052064.

[11] E. A. Ramírez, N. Béraud, F. Pourroy, F. Villeneuve, J. L. Amaya, M. Museau, “Design methodology of functionally graded cellular materials: Manipulating design parameters of triply periodic minimal surfaces through three-dimensional density

distributions," *Computer-Aided Design*, vol. 177, 103778, Dec. 2024, doi: 10.1016/j.cad.2024.103778.

[12] N. V. Viet, W. Waheed, A. Alazzam, W. Zaki, "Effective compressive behavior of functionally graded TPMS titanium implants with ingrown cortical or trabecular bone," *Composite Structures*, vol. 303, 116288, Jan. 2023, doi: 10.1016/j.compstruct.2022.116288.

[13] T. Szatkiewicz, D. Laskowska, B. Bałasz, K. Mitura, "The influence of the structure parameters on the mechanical properties of cylindrically mapped gyroid TPMS fabricated by selective laser melting with 316L stainless steel powder," *Materials*, vol. 15, no. 12, 4352, Jun. 2022, doi: 10.3390/ma15124352/s1.

[14] N. Wang, G. K. Meenashisundaram, S. Chang, J. Y. H. Fuh, S. T. Dheen, A. Senthil Kumar, "A comparative investigation on the mechanical properties and cytotoxicity of Cubic, Octet, and TPMS gyroid structures fabricated by selective laser melting of stainless steel 316L," *Journal of the Mechanical Behavior of Biomedical Materials*, vol. 129, 105151, May 2022, doi: 10.1016/j.jmbbm.2022.105151.

[15] C. M. Suryawanshi, S. Sagar, R. Bhallamudi, S. Mishra, "Effective design and mechanical response of Gyroid lattice scaffold for orthopedic implants," *Manufacturing Letters*, vol. 35, pp. 493–501, Aug. 2023, doi: 10.1016/j.mfglet.2023.07.015.

[16] M. Ozdemir, U. Simsek, G. Kiziltas, C. E. Gayir, A. Celik, P. Sendur, "A novel design framework for generating functionally graded multi-morphology lattices via hybrid optimization and blending methods," *Additive Manufacturing*, vol. 70, 103560, May 2023, doi: 10.1016/j.addma.2023.103560.

[17] S. Yu, J. Sun, J. Bai, "Investigation of functionally graded TPMS structures fabricated by additive manufacturing," *Materials & Design*, vol. 182, 108021, Nov. 2019, doi: 10.1016/j.matdes.2019.108021.

[18] M. Li, J. Jiang, W. Liu, X. Huang, X. Wu, W. Wei, H. Zhu, J. Zhang, J. Xiao, H. Dai, "Bioadaptable bioactive glass-β-tricalcium phosphate scaffolds with TPMS-gyroid structure by stereolithography for bone regeneration," *Journal of Materials Science & Technology*, vol. 155, pp. 54–65, Aug. 2023, doi: 10.1016/j.jmst.2023.01.025.

[19] A. Almesmari, N. Baghous, C. J. Ejeh, I. Barsoum, R. K. Abu Al-Rub, "Review of Additively Manufactured Polymeric Metamaterials: Design, Fabrication, Testing and Modeling," *Polymers*, Vol. 15, Page 3858, vol. 15, no. 19, 3858, Sep. 2023, doi: 10.3390/polym15193858.

[20] L. Yuan, S. Ding, C. Wen, "Additive manufacturing technology for porous metal implant applications and triple minimal surface structures: A review," *Bioactive Materials*, vol. 4, no. 1, pp. 56–70, Dec. 2019, doi: 10.1016/j.bioactmat.2018.12.003.

[21] W. Wu, D. Qi, H. Liao, G. Qian, L. Geng, Y. Niu, J. Liang, "Deformation mechanism of innovative 3D chiral metamaterials," *Scientific Reports*, vol. 8, no. 1, pp. 1–10, Aug. 2018, doi: 10.1038/s41598-018-30737-7.

[22] H. Ebrahimi, D. Mousanezhad, H. Nayeb-Hashemi, J. Norato, A. Vaziri, "3D cellular metamaterials with planar anti-chiral topology," Materials & Design, vol. 145, pp. 226–231, May 2018, doi: 10.1016/j.matdes.2018.02.052.

[23] Z. Wang, C. Luan, G. Liao, J. Liu, X. Yao, J. Fu, “Progress in auxetic mechanical metamaterials: structures, characteristics, manufacturing methods, and applications,” *Advanced Engineering Materials*, vol. 22, no. 10, 2000312, Oct. 2020, doi: 10.1002/adem.202000312.

[24] C. Ma, H. Lei, J. Liang, W. Wu, T. Wang, D. Fang, “Macroscopic mechanical response of chiral-type cylindrical metastructures under axial compression loading,” *Materials & Design*, vol. 158, pp. 198–212, Nov. 2018, doi: 10.1016/j.matdes.2018.08.022.

[25] T. Frenzel, M. Kadic, M. Wegener, “Three-dimensional mechanical metamaterials with a twist,” *Science*, vol. 358, no. 6366, pp. 1072–1074, Nov. 2017, doi: 10.1126/science.aao4640.

[26] **A. Vasile**, I. C. Coropetchi, D. M. Constantinescu, St.S. Sorohan, C. R. Picu, “A simulated annealing algorithm for stiffness optimization,” *Procedia Structural Integrity*, vol. 37, no. C, pp. 857–864, 2021, doi: 10.1016/j.prostr.2022.02.019.

[27] R. Ni, B. Qian, C. Liu, X. Liu, J. Qiu, “A cross-linking strategy with moderated pre-polymerization of resin for stereolithography,” *RSC Advances*, vol. 8, no. 52, pp. 29583–29588, 2018, doi: 10.1039/c8ra05432k.

[28] M. Ren, L. Wang, T. Li, B. Wei, “Molecular investigation on the compatibility of epoxy resin with liquid oxygen,” *Theoretical and Applied Mechanics Letters*, vol. 10, no. 1, pp. 38–45, Jan. 2020, doi: 10.1016/j.taml.2019.06.010.

[29] “Solid density of 3D-printed resin parts| Liqcreate.” Accessed: Nov. 28, 2024. [Online], https://www.liqcreate.com/supportarticles/solid-density-of-3d-printed-resin-parts-after-post-processing.

[30] A. Mukhangaliyeva, D. Dairabayeva, A. Perveen, D. Talamona, “Optimization of Dimensional Accuracy and Surface Roughness of SLA Patterns and SLA-Based IC Components,” *Polymers*, vol. 15, no. 20, 4038, Oct. 2023, doi: 10.3390/polym15204038.

[31] M. Mukhtarkhanov, A. Perveen, D. Talamona, “Application of Stereolithography Based 3D Printing Technology in Investment Casting,” *Micromachines*, vol. 11, no. 10, 946, Oct. 2020, doi: 10.3390/mi11100946.

[32] F. Emir, S. Ayyildiz, “Accuracy evaluation of complete-arch models manufactured by three different 3D printing technologies: a three-dimensional analysis,” *Journal of Prosthodontic Research*, vol. 65, no. 3, pp. 365–370, 2021, doi: 10.2186/jpr.jpor_2019_579.

[33] C. Arnold, D. Monsees, J. Hey, R. Schweyen, “Surface quality of 3D-printed models as a function of various printing parameters,” *Materials*, vol. 12, no. 12, Jun. 2019, doi: 10.3390/ma12121970.

[34] Y. Lu, A. J. Feilzer, L. Wang, A. M. O. Dal Piva, J. P. M. Tribst, I. Nedeljkovic, C. J. Kleverlaan, “Influence of surface finishing and printing layer orientation on surface roughness and flexural strength of stereolithography-manufactured dental zirconia,” *Journal of the Mechanical Behavior of Biomedical Materials*, vol. 143, 105944, Jul. 2023, doi: 10.1016/j.jmbbm.2023.105944.

Formatted: French (France)

[35] X. Zheng, Z. Li, F. Duan, Z. Song, H. Mo, Y. Song, Y. Su, X. Wang, “A TMPS-designed personalized mandibular scaffolds with optimized SLA parameters and mechanical properties,” *Frontiers in Materials*, vol. 9, 966031, Aug. 2022, doi: 10.3389/fmats.2022.966031/bibtex.

[36] **A. Vasile**, D. M. Constantinescu, I. C. Coropețchi, Ștefan. Sorohan, D. A. Apostol, “Assessment of the additive fabrication quality of sandwich structures with novel triply periodic minimal surface cores,” *Solids*, vol. 5, no. 4, pp. 665–680, Dec. 2024, doi: 10.3390/solids5040045.

[37] J. Zhang, S. Xie, T. Li, Z. Liu, S. Zheng, H. Zhou, “A study of multi-stage energy absorption characteristics of hybrid sheet TPMS lattices,” *Thin-Walled Structures*, vol. 190, 110989, Sep. 2023, doi: 10.1016/j.tws.2023.110989.

[38] M. F. Ashby, “The properties of foams and lattices,” *Philosophical Transactions of the Royal Society A: Mathematical, Physical and Engineering Sciences*, vol. 364, no. 1838, pp. 15–30, Jan. 2006, doi: 10.1098/rsta.2005.1678.

[39] **A. Vasile**, D. M. Constantinescu, I. C. Coropețchi, Șt. Sorohan, D. A. Apostol, “Definition, Fabrication, and Compression Testing of Sandwich Structures with Novel TPMS-Based Cores,” *Materials*, vol. 17, no. 21, 5150, Oct. 2024, doi: 10.3390/ma17215150.

[40] **A. Vasile**, I. C. Coropețchi, A. I. Indreș, D. M. Constantinescu, Șt. Sorohan, D. A. Apostol, “Response of sandwich structures with novel TPMS cores under cyclic uniaxial compression,” *Journal of Theoretical and Applied Mechanics*, vol. 63, Mar. 2025.

[41] **A. Vasile**, D. M. Constantinescu, A. I. Indreș, I. C. Coropețchi, Șt. Sorohan, D. A. Apostol, “Numerical simulation of compressive testing of sandwich structures with novel triply periodic minimal surface cores,” *Materials*, vol. 18, no. 2, 260, Jan. 2025, doi: 10.3390/MA18020260.

[42] M. T. Dehkordi, H. Nosraty, M. M. Shokrieh, G. Minak, D. Ghelli, “Low velocity impact properties of intra-ply hybrid composites based on basalt and nylon woven fabrics,” *Materials & Design*, vol. 31, no. 8, pp. 3835–3844, Sep. 2010, doi: 10.1016/j.matdes.2010.03.033.

[43] C. J. Ejeh, I. Barsoum, R. K. Abu Al-Rub, “Impact behavior of periodic, stochastic, and anisotropic minimal surface-lattice sandwich structures,” *International Journal of Mechanical Sciences*, vol. 276, 109359, Aug. 2024, doi: 10.1016/j.ijmecsci.2024.109359.

Formatted: French (France)